



Received: 04-02-2023
Accepted: 14-03-2023

International Journal of Advanced Multidisciplinary Research and Studies

ISSN: 2583-049X

The Evolutionary and Clinical Implications of Building an Archaeal Ribosome from a transfer RNA Fragment Ribozyme *In-Silico*

Bruce K Kowiatek

Blue Ridge Community and Technical College, Martinsburg, WV, USA

Corresponding Author: Bruce K Kowiatek

Abstract

Tandem repeats of non-coding, but occasionally coding chromosome sequences of one kilo-base-pair (kb) nucleotides (nts) or greater in deoxyribonucleic acid (DNA) and ribonucleic acid (RNA), are found in the genomes of organisms in all three kingdoms of life, oftentimes crossing over from one kingdom to another. Indeed, hyper- and/or hypomethylation of these tandem repeat sequences has been associated with several human disease states, including cancer, schizophrenia, Facioscapulohumeral Muscular Dystrophy (FSHD), and Immunodeficiency, Centromeric Instability, and facial anomalies (ICF).

Since transfer RNA (tRNA) is becoming more widely

accepted as the first genetic material, evolving from a ribozyme, with ribosomal RNA (rRNA) in turn evolving from it, an *in-silico* study was performed using prokaryotic genomic tRNA to assess whether or not tandem repeats of archaeal tRNA fragment ribozyme polymers could serve as viable 16S, 23S, and 5S subunits of ribosomes. The results not only indicate that they can, but that only one tRNA fragment ribozyme type is needed to do so. The evolutionary implications of this, as well as the clinical use of a widely used nt methylator were then evaluated, with the results and conclusions also reported herein.

Keywords: tRNA, Ribosome, Archaea, Tandem Repeat Sequence, L-alanine

Introduction

Tandem repeats of non-coding, but occasionally coding chromosome sequences of one kilo-base-pair (kb) nucleotides (nts) or greater in deoxyribonucleic acid (DNA) and ribonucleic acid (RNA), are found in the genomes of organisms of all three kingdoms of life, oftentimes crossing over from one kingdom to another ^[1]. Indeed, hyper- and/or hypomethylation of these tandem repeat sequences has been associated with several human disease states, including cancer ^[2], schizophrenia ^[3], Facioscapulohumeral Muscular Dystrophy (FSHD) ^[4], and Immunodeficiency, Centromeric Instability, and facial anomalies (ICF) ^[5].

Since transfer RNA (tRNA) is becoming more widely accepted as the first genetic material, evolving from a ribozyme ^[6], with ribosomal RNA (rRNA) in turn evolving from it ^[7], an *in-silico* study was performed using prokaryotic genomic tRNA to assess whether or not tandem repeats of archaeal tRNA fragment ribozyme polymers could serve as viable 16S, 23S, and 5S subunits of ribosomes. The results not only indicate that they can, but that only one tRNA fragment ribozyme type is needed to do so. The evolutionary implications of this, as well as the clinical use of a widely used nt methylator were then evaluated, with the results and conclusions also reported herein.

Methodology

The ribozyme-containing tRNAs of the archaeon *Methanobrevibacter ruminantium* (*M. ruminantium*) were surveyed using the Kyoto Encyclopedia of Genes and Genomes (KEGG) (<https://www.genome.jp/kegg/>) database for those whose ribozyme fragments formed polymers when input into the NCBI Nucleotide Blast (https://blast.ncbi.nlm.nih.gov/Blast.cgi?PROGRAM=blastn&PAGE_TYPE=BlastSearch&LINK_LOC=blasthome) database via Blastn queries. *M. ruminantium* was selected due to its representative quality of the thermophilic methanogens, regarded as one of the most ancient life forms on Earth ^[8], closest to the Last Universal Common Ancestor (LUCA) (Fig 1). Heat-driven tRNA replicative polymerization based upon its hairpin structure has also recently been successfully modeled ^[9]. Fig 2 illustrates this process, with the rationale that a hairpin tRNA ribozyme fragment would polymerize similarly, an assertion supported by this modeling.

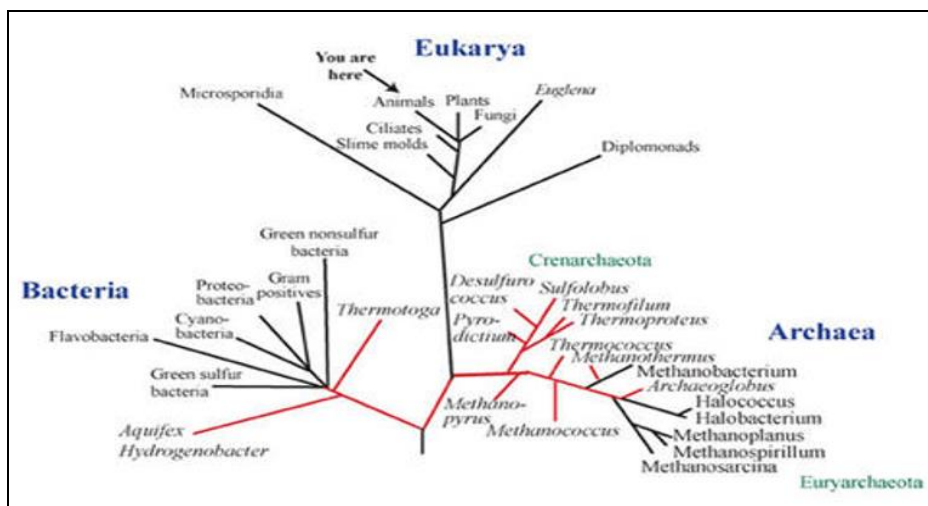


Fig 1: Detailed Phylogenetic Tree of *Archaea*, *Bacteria*, and *Eukarya*. Note the proximity of the methanogens to the central tree “trunk” representing the path to LUCA

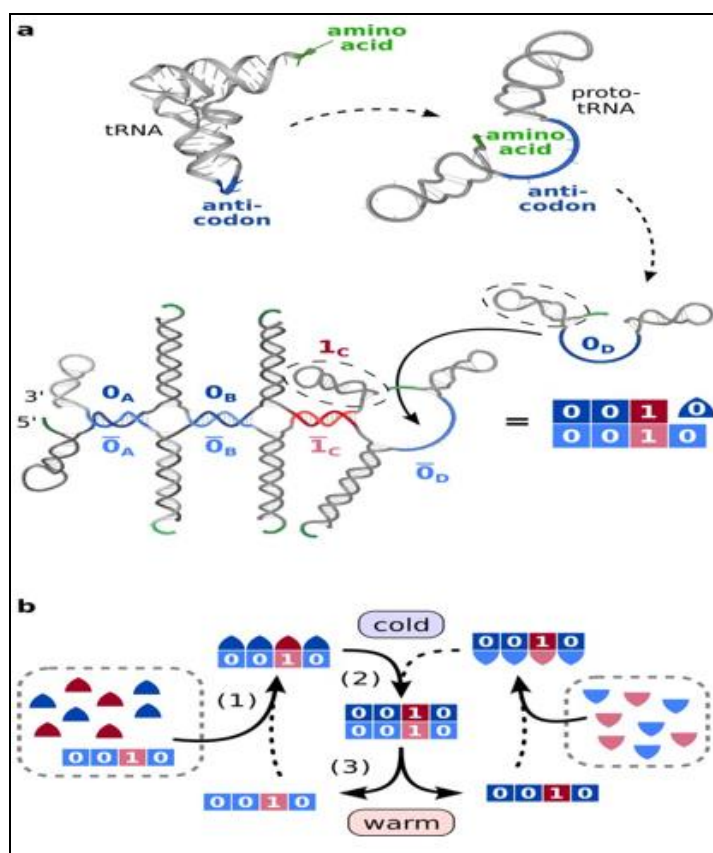


Fig 2: Heat-driven replication by hybridization using hairpin structures inspired from transfer RNA

(a) Transfer RNA folds into a double-hairpin conformation upon very few base substitutions. In that configuration, the 3'-terminal amino acid binding site (green) is close to the anticodon (blue) and a double hairpin structure forms. A set of pairwise complementary double hairpins can encode and replicate sequences of information. A binary code implemented in the position of the anticodon, the information domain, allows to encode and replicate binary sequences (red vs blue). Each strand (82-84 nt) comprises two hairpin loops (gray) and an interjacent unpaired information domain of 15 nt length (blue/red, here: 0D). The displayed structure of eight strands shows replication of a template corresponding to the binary code 0010. Note that no covalent linkage

is involved in the process.
 (b) Replication is driven by thermal oscillations in four steps: (0) The hairpins are activated into their closed conformation by fast cooling indicated by triangles. (1) Strands with matching information domain bind to the template. (2) Fluctuations in the bound strands' hairpins facilitate the hybridization of neighboring strands. (3) Subsequent heating splits replica from template, while keeping the longer hairpin sequences connected, freeing both as templates for the next cycle.

The Blastn results of the longest polymers observed for *M. ruminantium* tRNAs and any corresponding fragment ribozymes are summarized in Table 1.

Table 1

tRNA	Polymer Length (kb)	Expect Value	% of Identities	% of Gaps
tRNA ^{Asn(GUU)} <i>M. ruminantium</i> : 86-nt	12.0	0.00**	68	4
tRNA ^{Asn(GUU)} <i>M. ruminantium</i> : 42-nt fragment ribozyme	42.0	0.00**	65	6
tRNA ^{Ile(GAU)} <i>M. ruminantium</i> : 75-nt	3.4	1 e - 131	68	6
tRNA ^{Ala(UGC)} <i>M. ruminantium</i> : 73-nt	1.5	2 e - 43	66	10
tRNA ^{Ala(UGC)} <i>M. ruminantium</i> : 47-nt fragment ribozyme	2.0	4 e - 19	67	20

** Denotes a Blastn Expect Value exceedingly less than 1, usually for polymers > 5.0 kb

Although the L-asparagine tRNA^{Asn(GUU)} proved to form the longest polymers, with its 42-nt fragment ribozyme forming an astounding 42.0 kb tandem repeat, neither of them matched any Blastn hits corresponding to any ribosomal subunit or intergenic spacer sequences between subunits. Both the L-isoleucine tRNA^{Ile(GAU)} and L-alanine tRNA^{Ala(UGC)} on the other hand matched with Blastn hits corresponding to intergenic spacer rRNA sequences between prokaryotic 16S, 23S, and 5S rRNA subunits, a fact that has been known for some time now, since the early 1980s^[10].

Due to the lack of a tRNA fragment ribozyme derived from tRNA^{Ile(GAU)}, the 47-nt tRNA^{Ala(UGC)} fragment ribozyme (Fig 3) was chosen as the sole fragment ribozyme from which to attempt to polymerize the 16S, 23S, and 5S rRNA subunits. Interestingly, while both tRNA^{Ile(GAU)} and tRNA^{Ala(UGC)} are found in prokaryotic intergenic spacer regions between subunits as previously mentioned, only tRNA^{Ala(UGC)} returned any Blastn hits corresponding to the prokaryotic rRNA subunits themselves.

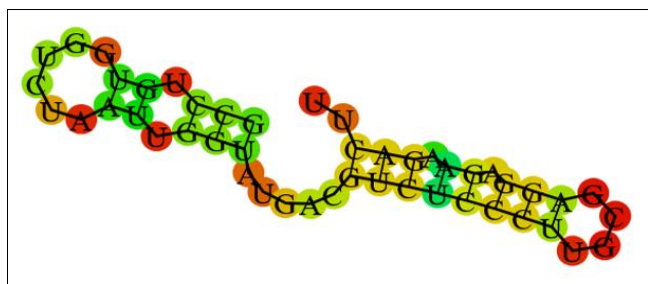


Fig 3: 47-nt tRNA^{Ala(UGC)} fragment ribozyme (image generated from RNAFold WebServer (http://rna.tbi.univie.ac.at/cgi-bin/RNAWebSuite/RNAfold.cgi?PAGE=3&ID=xKgwbj6z_Z))

A 47-nt tandem repeat sequence (GCCUGUGGUCUAAUUGGUAUGACGUCUCCCUUGCGAGGAGAAGACUU) of tRNA^{Ala(UGC)} fragment ribozyme polymers were then input into the NCBI Nucleotide Blast database in order to see if there were any matches which corresponded to the positioning of the universal catalytic A- and P-site nts in the ribosomal Peptidyl Transferase Center (PTC), common to all ribosomes, with G530, A1492, and A1493 being essential in

the 1540-nt 16S rRNA subunit^[11] (Fig 4), and G2284 (2251), G2285 (2252), G2286 (2253), A2485 (2450), A2486 (2451), G2588 (2553), U2589 (2554), and U2590 (2555) being essential in the 2900-nt 23S rRNA subunit^[12] (Fig 5).

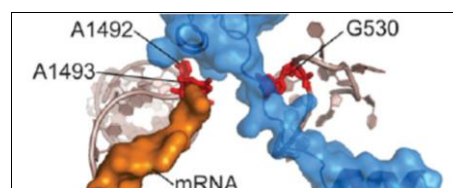


Fig 4: Messenger RNA (mRNA) and aminoacylated tRNA (on the right, unlabeled) passing through the catalytic A- and P-sites of the prokaryotic 16S rRNA subunit. Note the essential nts G530, A1492, and A1493

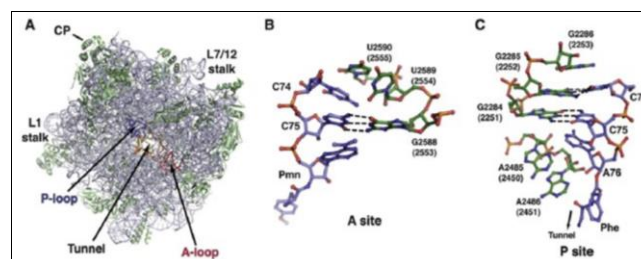


Fig 5: The structure of the ribosomal PTC and the mode of tRNA recognition. (A) A cartoon diagram of the 23S subunit from *M. ruminantium* showing the exact location of the PTC. The two-fold symmetry of the active site is evident. The P loop is blue, the A loop is red, whereas the floor and the walls of the PTC are orange. The arrow points to the tunnel entrance. rRNA is light blue, while the proteins are colored in light green. (B) The A loop (green) binds CCA of the A-site substrate analog CC-Pmn (blue). C75 makes Watson-Crick interactions with G2588 (G2553) and C75 base stacks with U2590 (U2555). (C) The P-loop (green) bases G2285 (G2252) and G2284 (G2251) form Watson-Crick base pairs with C74 and C75 of the peptidyl-tRNA mimic CCA-Pcb (blue), respectively. In A and B hydrogen bonds are shown with dashed lines

Results

The 5S rRNA Database (<http://combio.pl/rRNA/>) was queried for the *M. ruminantium* 130-nt sequence and found to structurally correspond to an *M. ruminantium* 63-nt tRNA^{Ala(UGC)} fragment ribozyme (Fig 6).

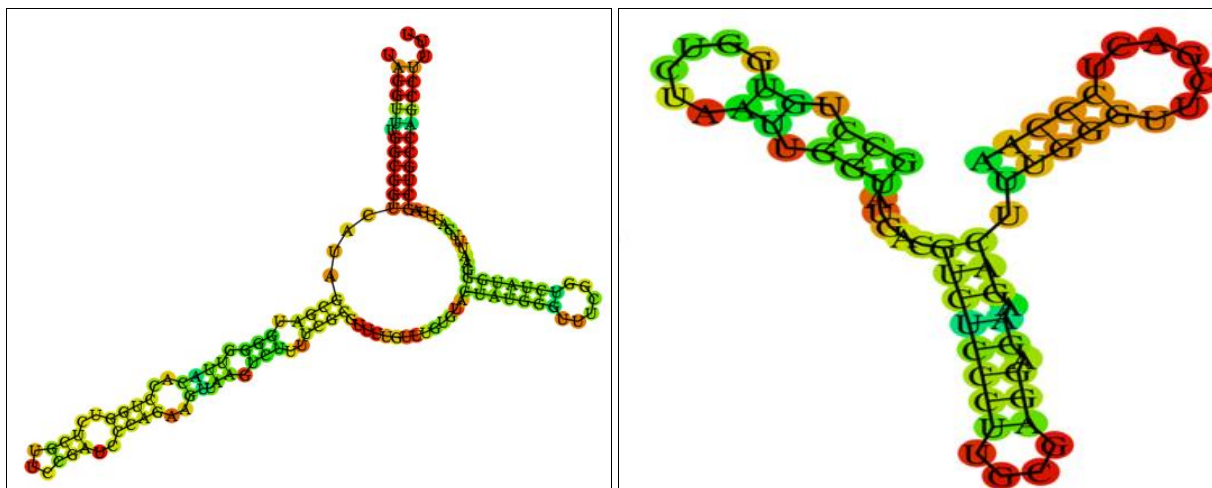


Fig 6: Left: 130-nt *M. ruminantium* 5S rRNA subunit. Right: Structurally similar *M. ruminantium* 63-nt tRNA^{Ala(UGC)} fragment ribozyme. Both generated from RNAFold WebServer (http://rna.tbi.univie.ac.at/cgi-bin/RNAWebSuite/RNAfold.cgi?PAGE=3&ID=xKgwbj6z_Z)

Similarly, polymers of 31 and 59 tandem repeats of the 47-nt *M. ruminantium* tRNA^{Ala(UGC)} fragment ribozyme yielded structurally similar results compared to the *M. ruminantium*

16S and 23S ribosomal subunits, respectively, including positioning of previously mentioned catalytic active site nts. (Fig 7 and 8).

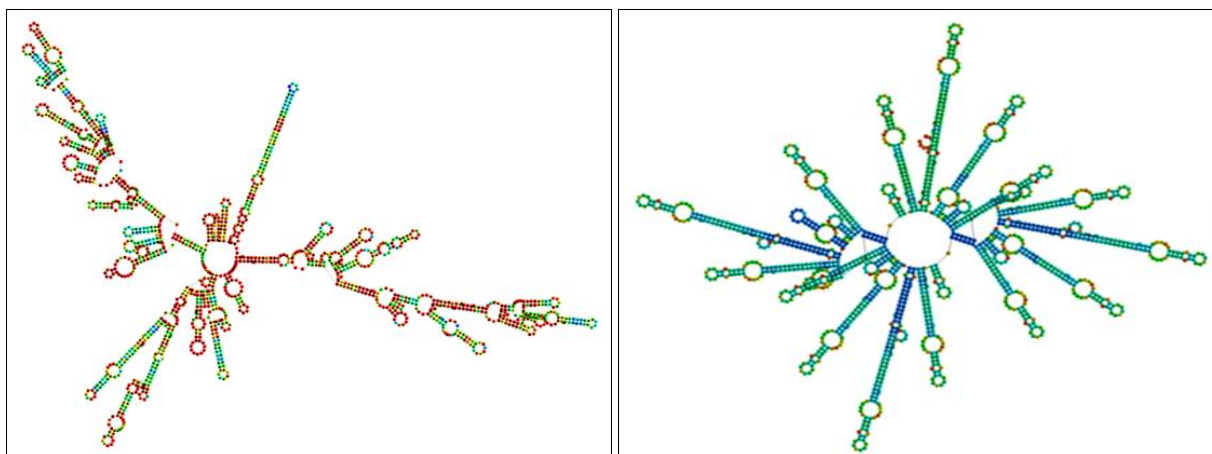


Fig 7: Left: *M. ruminantium* 16S ribosomal subunit from RFam RNA Family Database (<https://rfam.org/family/RF01959#tabview=tab3>). Right: *M. ruminantium* tRNA^{Ala(UGC)} fragment ribozyme 31-mer polymer generated from RNAFold WebServer (http://rna.tbi.univie.ac.at/cgi-bin/RNAWebSuite/RNAfold.cgi?PAGE=3&ID=xKgwbj6z_Z). Note same positioning of active catalytic sites: upper center closed red circle on left and upper open red semicircle on right

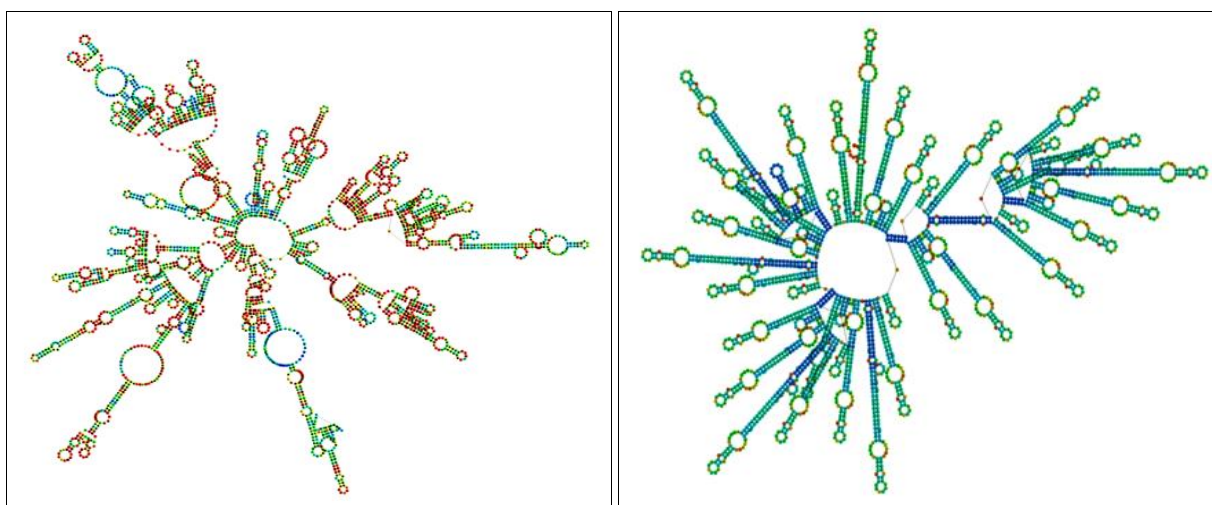


Fig 8: Left: *M. ruminantium* 23S ribosomal subunit from RFam RNA Family Database (<https://rfam.org/family/RF01959#tabview=tab3>). Right: *M. ruminantium* tRNA^{Ala(UGC)} fragment ribozyme 59-mer polymer generated from RNAFold WebServer (http://rna.tbi.univie.ac.at/cgi-bin/RNAWebSuite/RNAfold.cgi?PAGE=3&ID=xKgwbj6z_Z). Note same positioning of active catalytic sites: upper center closed red circle on left and upper open red semicircle on right

Remarkably, the *M. ruminantium*, 31 tandem repeat sequences of the tRNA^{Ala(UGC)} fragment ribozyme polymer, when run through the NCBI Nucleotide Blast database, yielded a nt positioning match of 100% of the previously discussed essential 16S rRNA subunit nts, allowing for genetic drift with a statistical F-value of ± 1 nt^[13].

Just as remarkably, the *M. ruminantium*, 59 tandem repeat sequences of the tRNA^{Ala(UGC)} fragment ribozyme polymer, when run through the NCBI Nucleotide Blast database, yielded a nt positioning match of 100% of the previously

discussed essential 23S rRNA subunit nts, allowing for genetic drift with a statistical F-value of ± 1 nt^[13].

Fig 9 illustrates the near-perfect alignment between the *M. ruminantium* ribosome, and a Graphic Summary of the sequences proposed herein when run through the NCBI Nucleotide Blast database, that also includes an intergenic spacer tRNA^{Ala(UGC)} between the 16S and 23S rRNA subunits and a terminal L-cysteine tRNA^{Cys(GCA)} residue. Expect Value is 4e-19 with 67% Identities and 20% Gaps.

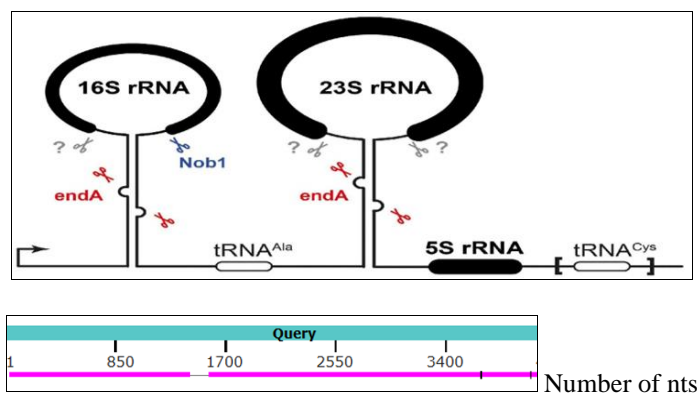


Fig 9: Near-perfect alignment between the *M. ruminantium* ribosome and a Graphic Summary of the sequences proposed herein when run through the NCBI Nucleotide Blast database, that also includes an intergenic spacer tRNA^{Ala(UGC)} between the 16S and 23S rRNA subunits and a terminal L-cysteine tRNA^{Cys(GCA)} residue. Expect Value is 4e-19 with 67% Identities and 20% Gaps

Discussion

With the *M. ruminantium* 31 and 59 tandem repeat sequences of the tRNA^{Ala(UGC)} fragment ribozyme polymers, along with the 63-nt tRNA^{Ala(UGC)} fragment ribozyme sequence so structurally similar to the *M. ruminantium* 16S, 23S, and 5S rRNA subunits, respectively, taken together with the 100% positioning matches of the essential nts necessary to form the catalytic PTC for protein synthesis and the near-perfect alignment between the proposed sequences and the *M. ruminantium* ribosome, all factor into indicating the proper folding of nts to produce viable subunits, resulting in a viable ribosome.

Conclusion

With the evolutionary accretion model of the ribosome forming around a central ribozyme acting as the PTC^[14] being ever more widely accepted, along with the mounting evidence of a ribozyme origin for tRNA, and rRNA's

subsequent evolution from that, these findings may very well indicate the nature of the initial ribozyme responsible for beginning the entire process. Further research into this possibility is thus clearly warranted.

Prospectus

Returning to the topic of the hyper- and/or hypomethylation of tandem repeat nt sequences being implicated in various human disease states, particularly cancer, mention should be made that, with cancer, a global hypomethylation condition exists^[15]. In 2019, the recommendation was made to add the over-the-counter (OTC) supplement s-adenosylmethionine (Sam-E), the chief intracellular methylator in living organisms, as an adjuvant treatment to chemotherapy and radiation therapy^[16]. Since that time, the successful use of this protocol in the treatment of chronic lymphocytic leukemia (CLL) has nearly doubled (Fig 10).

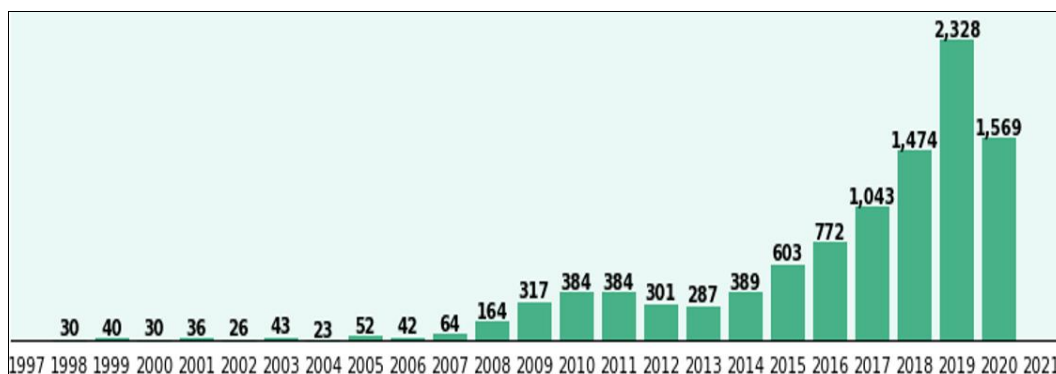


Fig 10: U.S. Nationwide Implementation of Protocol First-Line as per the U.S. FDA (https://www.ehealthme.com/compare-drugs/3615/). 10,401 females aged 54 (±5) who take Sam-E, Bendamustine, Rituxan for CLL are studied. Number of reports submitted per year with Very High Effectiveness

The clinical recommendation is now put forth to expand this use of Sam-E as an adjuvant therapy in all of the conditions previously listed to address their inherent nt hypomethylation issues. Its highly successful and effective application thus far warrants such expanded use, beginning at the very least with case studies, as this one did, and branching out from there. The potential boon to help alleviate human suffering may in time prove to be incalculable.

Acknowledgements

I especially thank my loving family for their generous gift of time in the writing of this paper, as well as my fellow faculty and staff at Blue Ridge Community and Technical College (BRCTC).

Conflict of Interest Statement

The author declares no conflict of interest in the performance of this research or the writing of this paper.

References

1. Hadjiargyrou M, Delihias N. The Intertwining of Transposable Elements and Non-Coding RNAs International Journal of Molecular Sciences. 2013; 14(7):13307-13328. Doi: <https://doi.org/10.3390/ijms140713307>
2. Nishiyama R, Qi L, Tsumagari K, Weissbecker K, Dubeau L, Champagne M, *et al.* A DNA repeat, NBL2, is hypermethylated in some cancers but hypomethylated in others, Cancer Biology & Therapy, 2005, 4:4:446-454. Doi: 10.4161/cbt.4.4.1622
3. Li S, Yang Q, Hou Y, Jiang T, Zong L, Wang Z, *et al.* Hypomethylation of LINE-1 elements in schizophrenia and bipolar disorder. J Psychiatr Res. 2018; 107:68-72. Doi: 10.1016/j.jpsychires.2018.10.009. Epub 2018 Oct 10. PMID: 30326341. <https://pubmed.ncbi.nlm.nih.gov/30326341/>
4. Salsi V, Magdinier F, Tupler R. Does DNA Methylation Matter in FSHD? Genes (Basel). 2020; 11(3):258. Doi: 10.3390/genes11030258. PMID: 32121044; PMCID: PMC7140823. <https://www.ncbi.nlm.nih.gov/pmc/articles/PMC7140823/>
5. Robertson, KD. Immunodeficiency, Centromeric Instability and Facial Anomalies (ICF) Syndrome: A Disease of DNA Methylation. Mayo Clinic Laboratories Epigenetic Etiology of Human Disease, 2023. <https://www.mayo.edu/research/labs/epigenetic-etiology-human-disease/research/immunodeficiency-centromeric-instability-facial-anomalies-syndrome>
6. Kim Y, Kowiatek B, Opron K, Burton ZF. Type-II tRNAs and Evolution of Translation Systems and the Genetic Code. Int J Mol Sci. 2018; 19(10):3275. Doi: 10.3390/ijms19103275. PMID: 30360357; PMCID: PMC6214036.
7. De Farias, ST Rêgo TG, José MV. TRNA Core Hypothesis for the Transition from the RNA World to the Ribonucleoprotein World. Life. 2016; 6(2):15. Doi: <https://doi.org/10.3390/life6020015>
8. Zhenbo L, Ding J, Wang H, Wan J, Chen Y, Liang L, *et al.* Isolation of a Novel Thermophilic Methanogen and the Evolutionary History of the Class Methanobacteria. Biology. 2022; 11(10):1514. Doi: <https://doi.org/10.3390/biology11101514>
9. Kühnlein A, Lanzmich SA, Braun D. tRNA sequences can assemble into a replicator. eLife. 2021; 10:e63431.
10. Loughney K, Lund E, Dahlberg JE. tRNA genes are found between 16S and 23S rRNA genes in *Bacillus subtilis*. Nucleic Acids Res. 1982; 10(5):1607-24. Doi: 10.1093/nar/10.5.1607. PMID: 6280153; PMCID: PMC320553.
11. Abdi NM, Fredrick K. Contribution of 16S rRNA nucleotides forming the 30S subunit A and P sites to translation in *Escherichia coli*. RNA. 2005; 11(11):1624-1632. Doi: 10.1261/rna.2118105. Epub 2005 Sep 21. PMID: 16177132; PMCID: PMC1370848.
12. Simonovic M, Steitz T. A structural view on the mechanism of the ribosome-catalyzed peptide bond formation. Biochimica, 2009.
13. Na. F-value. IBM. Ref, 2023. <https://www.ibm.com/docs/no/cognos-analytics/11.1.0?topic=terms-f-value>
14. Cech TR. Structural biology. The ribosome is a ribozyme. Science. 2000; 289(5481):878-9. Doi: 10.1126/science.289.5481.878. PMID: 10960319.
15. Ehrlich M. DNA hypomethylation in cancer cells. Epigenomics. 2009; 1(2):239-259.
16. Kowiatek BK. Non-enzymatic Methylation of Cytosine in RNA by S-adenosylmethionine and Implications for the Evolution of Translation. Journal of Biotechnology and Biomedicine. 2019; 2:48-56.